Development and Investigation of Mathematical Model of an Optoelectronic Sensor of Methane Concentration

Oleksandr Volodymyrovych VOVNA, Ivan Serhiiovych LAKTIONOV, Anatolii Anatoliiovych ZORI, Ramin Nizamiiovych AKHMEDOV

Department of Electronic Engineering, Faculty of Computer-Integrated Technologies, Automatization, Electrical Engineering and Radioelectronics, State Higher Educational Establishment Donetsk National Technical University, Shybankova Square 2, 85300 Pokrovsk, Donetsk region, Ukraine

oleksandr.vovna@donntu.edu.ua, ivan.laktionov@donntu.edu.ua, anatolii.zori@donntu.edu.ua, ramin.akhmedov@donntu.edu.ua

DOI: 10.15598/aeee.v16i3.2847

Abstract. *A mathematical model of a methane concentration sensor has been developed and studied, which takes into account the use of materials with different optical properties in the channel, spectral and spatial adjustment of the sensor components, losses at modulation and signal processing, as well as scattering and absorption of the optical emission flux in the channel. Taking into account results of modelling and experimental studies of the prototype sensor, confirming the adequacy of the proposed model, types of optoelectronic sensor components, as well as its design parameters with allowable deviations in manufacturing, have been substantiated and selected. The emission losses in the optical channel have been minimized when the informative parameter is maximized, which is absorption of optical emission by the measured methane concentration, by providing the length of the sensor measuring channel not more than 30 mm and the use of light and photodiodes with covering of their sensitive elements with chalcogenide glass. It has been established that the main measurement error of methane concentration with the application of these recommendations is not more than 0.04* $^{vol.}$*% with the regulated value of 0.20* $^{vol.}$*% in the range from 0 to 5* $^{vol.}$*%, which significantly exceeds metrological characteristics of the existing prototypes of the methane concentration sensor for coal mine atmosphere.*

Keywords

Chalcogenide glass, concentration, measurement error, methane, optical path length, optoelectronic sensor.

1. Introduction

Methane is not only a gas that causes the greenhouse effect, but is also highly explosive under the influence of certain external forces. Currently, methane emission control means are being developed to minimize methane emissions [1]. Optoelectronic sensors [2] and [3] that have low sensitivity to the influence of destabilizing factors, fast response time and accuracy of measurement are widely used. There is a need for continuous improvement of methane concentration sensors in real time mode to ensure occupational safety in conditions of increased explosion hazard in coal mines [4].

One of the ways of improving methane concentration sensors is improving accuracy of measurement while maintaining the regulated speed [5]. The implementation of modern technologies for methane concentration measurement in coalmine conditions allows making the transition from the phenomenological approach to identifying and preventing explosive situations to the use of quantitative monitoring methods based on the results of mathematical modelling with subsequent laboratory tests. Therefore, development and research of mathematical models of the optoelectronic sensor of methane concentration is a topical scientific and applied problem, the solution of which will solve the problem of performing measurements on-line with the reduction of the influence of destabilizing factors and ensuring the regulated accuracy of measurements.

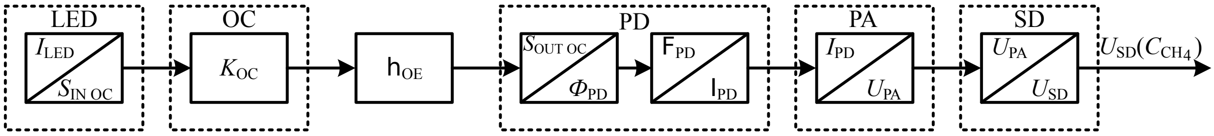

Fig. 1: Functional diagram of the optoelectronic methane concentration sensor.

2. Materials and Methods

The operating principle of the developed sensor is based on emission absorption in the Optical Channel (OC). The change in intensity of output signal of the optical channel ($\Delta I_{\mathrm{OUT\ OC}}$), path length ($l$, m) and methane concentration ($C_{\mathrm{CH_4}}$) is described by the Bouguer-Lambert-Beer law [6] and [7]:

$$\Delta I_{\mathrm{OUT\ OC}} = \Delta I_{\mathrm{IN\ OC}} \cdot e^{-\alpha_{CS}(\lambda,T,P)\cdot C_{\mathrm{CH_4\ M}}\cdot l}, \quad (1)$$

where $\Delta I_{\mathrm{IN\ OC}}$, W·sr^{-1} - change in intensity of input signal of the OC; $C_{\mathrm{CH_4\ M}}$, mole·cm^{-3} – molar methane concentration in the sensor OC; $\alpha_{CS}(\lambda, T, P)$ – coefficient of cross-section of the absorption spectrum of optical emission by methane, the value of which depends on temperature (T) and pressure (P) of the gas mixture being analysed [8]; λ, µm – wavelength of spectral lines of optical emission.

To analyse design parameters of the OC sensor, we recommend using emission flux density ($D_{\mathrm{CH_4}}$):

$$D_{\mathrm{CH_4}} = \alpha_{CS}(\lambda, T, P) \cdot C_{\mathrm{CH_4\ M}} \cdot l. \quad (2)$$

The sensor should measure volumetric methane concentration ($C_{\mathrm{CH_4\ v}}$, $^{\mathrm{vol.}}\%$), therefore, in the developed prototype recalculation in $C_{\mathrm{CH_4\ M}}$ was used [6]:

$$C_{\mathrm{CH_4\ M}} = \frac{C_{\mathrm{CH_4\ v}} \cdot P}{100 \cdot R \cdot T} \cdot 10^{-6}, \quad (3)$$

where R, J·mole^{-1}·K^{-1} - gas constant.

Taking into account Eq. (3), $D_{\mathrm{CH_4}}$ is equal to:

$$D_{\mathrm{CH_4}} = \alpha_{CS}(\lambda, T, P) \cdot \frac{C_{\mathrm{CH_4\ v}} \cdot P}{100 \cdot R \cdot T} \cdot 10^{-6} \cdot l. \quad (4)$$

When using Eq. (1), Eq. (2) and Eq. (4), the transmission coefficient of the optical channel K_{OC} (see Fig. 1) is equal to the ratio of $\Delta I_{\mathrm{OUT\ OC}}$ to $\Delta I_{\mathrm{IN\ OC}}$:

$$K_{\mathrm{OC}} = \exp\left(-\alpha_{CS}(\lambda, T, P) \cdot \frac{C_{\mathrm{CH_4\ v}} \cdot P}{100 \cdot R \cdot T} \cdot 10^{-6} \cdot l\right). \quad (5)$$

Analysis of Eq. (5) shows that K_{OC} is a nonlinear function of five variables, three of which ($C_{\mathrm{CH_4\ v}}, T, P$) characterize the state of the analysed gas environment. To ensure the regulated accuracy of the optoelectronic sensor, it is necessary to provide minimal emission losses in its optical unit, which will allow obtaining the maximum value of K_{OC}.

2.1. Aims and Objectives of the Study

The purpose of the study is to develop and implement recommendations for increasing accuracy of methane concentration measurement for production conditions of coal mines by improving the design parameters of the optoelectronic sensor based on the results of mathematical modelling while minimizing emission losses in the sensor optical channel. To achieve the goal, the following tasks were set and solved:

- to develop and investigate the mathematical model for estimating losses of optical emission flux, taking into account destabilizing factors in the sensor channel;
- to justify and develop recommendations for improving design parameters of the sensor to increase accuracy of methane concentration measurement.

2.2. Functional Diagram of the Sensor

When designing the optoelectronic methane concentration sensor, the functional diagram of which is shown in Fig. 1, a Light-Emitting Diode (LED) and a Photodiode (PD) were used, made in a uniform technological design with an Optical Channel (OC). The LED converts the supply current (I_{LED}) into a proportional value of optical power density (S_{LED}), which is fed to the OC input ($S_{\mathrm{IN\ OC}}$) [9]:

$$S_{\mathrm{IN\ OC}} = S_{LED} = S_{0LED} \cdot s_{LED}, \quad (6)$$

where s_{LED} – normalized spectral density of optical emission power of the LED; S_{0LED} – maximum value of S_{LED}.

Spectral density of the optical emission power of the OC output signal ($S_{\mathrm{OUT\ OC}}$) is determined to take into account $S_{\mathrm{IN\ OC}}$ calculated according to Eq. (6) and K_{OC} calculated by Eq. (5):

$$S_{\mathrm{OUT\ OC}} = S_{\mathrm{IN\ OC}} \cdot K_{\mathrm{OC}}. \quad (7)$$

The mathematical model of the methane concentration sensor was developed based on the optical electronic efficiency coefficient (η_{OE}). This coefficient determines a part of the useful signal that arrives at the sensor input and is used to obtain its informative component. The value of the sensor η_{OE} depends on the following destabilizing factors:

- use of materials with different optical properties, which is taken into account by the emission transmission coefficient (τ_O),
- spectral adjustment of the LED and PD, which is taken into account by coefficient k_λ,
- spatial adjustment of geometric dimensions of the PD with the parameters of the LED optical flow, which is taken into account by coefficient k_{XY},
- losses at modulation and the modulated signal processing, which is taken into account by modulation coefficient (k_M),
- dispersion of the emission flux with increasing l, which is taken into account by coefficient of emission input (k_{input}) into the PD window.

Influence of the listed destabilizing factors determines the sensor η_{OE}:

$$\eta_{\text{OE}} = \tau_O \cdot k_\lambda \cdot k_{XY} \cdot k_M \cdot k_{input}. \tag{8}$$

Consistent with η_{OE} calculated according to Eq. (8), $S_{\text{OUT OC}}$ is determined:

$$S_{\text{OUT OC}} = S_{IN\ \text{OC}} \cdot K_{\text{OC}} \cdot \eta_{\text{OE}}. \tag{9}$$

The process of converting the OC output signal ($S_{\text{OUT OC}}$) calculated by Eq. (9) into optical stream (ϕ_{PD}) and output current signal (I_{PD}) is carried out by the PD, which is described by the dependence:

$$I_{PD} = k_{\Phi\to I} \cdot \phi_{PD} = k_{\Phi\to I} \cdot \int_{\lambda_1}^{\lambda_2} S_{\text{OUT OC}} \text{d}\lambda, \tag{10}$$

where λ_1 and λ_2 – wavelength range of the LED; $k_{\Phi\to I}$ – conversion coefficient of optical emission flux (ϕ_{PD}) entering the PD input into a proportional current value (I_{PD}).

The sensor includes a Preamplifier (PA) of the PD output signal converting I_{PD}, the value of which is calculated by Eq. (10), into a voltage value (U_{PA}) followed by amplification, which is described by the dependence:

$$U_{PA} = k_{U\ PA} \cdot I_{PD} \cdot R_{in\ PA}, \tag{11}$$

where $R_{in\ PA}$, Ω– feed impedance PA; $k_{U\ PA}$ – voltage transfer coefficient PA.

To measure the amplitude value of the U_{PA} calculated according to Eq. (11), a Synchronous Detector (SD) is used in the optoelectronic sensor circuit, the signal conversion process in which is described by the dependence:

$$U_{SD} = k_{U\ SD} \cdot U_{PA}, \tag{12}$$

where $k_{U\ SD}$ – voltage transfer coefficient SD.

Thus, to assess metrological characteristics and parameters of the methane concentration sensor, it is necessary to develop a mathematical model of processes of changing the emission flux magnitude in the sensor.

3. Results and Discussion

Modelling of the influence of destabilizing factors on the value of optical electronic efficiency of the methane concentration sensor will allow developing recommendations for minimizing emission loss in the sensor optical channel and improving its design parameters, as well as increasing accuracy of methane concentration measurement.

3.1. Model of Emission Flux Losses in the Sensor

In the optical system, the main emission losses happen due to reflection at medium boundaries, as well as absorption in materials. That loss is accounted for by a transmission coefficient that takes into account loss of absorption and reflection:

$$\tau_{\text{O}} = \prod_{k=1}^{N} (1 - \rho_k), \tag{13}$$

where N – number of boundary surfaces; ρ_k – reflection coefficient at the k-th boundary surface of the optical medium.

The main components of the sensor, whose optical circuit is shown in Fig. 2, are the Optical Channel (OC), which has a length l, the LED and PD with focusing lenses (L_1 and L_2). The choice of the LED and PD is based on adjusting the spectrum of methane absorption in the OC with spectral characteristics of these optoelectronic components. As the emission source of the sensor, Lms34LED-CG LED [10] with a central emission wavelength of 3.4 μm is used, which corresponds to the maximum intensity of the spectral absorption lines of methane [8]. The receiver of the emission is Lms36PD-CG PD [11], as its spectral characteristics are the closest and consistent with the spectral characteristics of Lms34LED-CG LED.

More than 20 years scientists from Infrared optoelectronics Laboratory of the Ioffe Institute in collaboration with IBSG Co.Ltd work under creation of high-efficiency emitters and detectors based on narrow

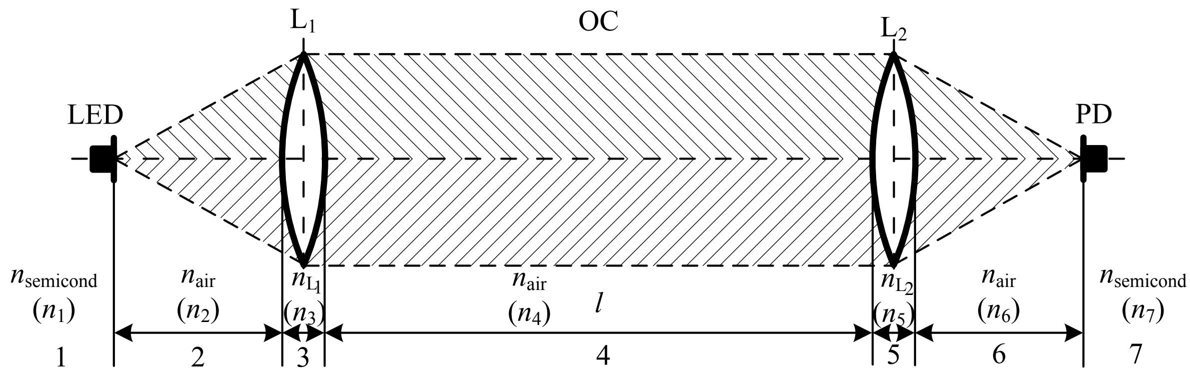

Fig. 2: Optical diagram of the measuring channel of the methane concentration sensor.

band-gap III-V semiconductors. Qualitative technological break-through in heterostructure growing based on GaInAsSb solid solution was achieved in the last decade. This material system allows developing of LEDs, Laser Diodes and Photodiodes that cover wide spectral range from 1600 nm to 5000 nm. Using GaInAsSb/AlGaAsSb heterostructures lattice matched to GaSb substrate allowed us to create LEDs and PDs for 1.6 – 2.4 μm spectral range, InAsSb/InAsSbP lattice matched to InAs substrate – for 2.8 – 5.0 μm spectral range [10] and [11].

The emission fluxes enter the interface between the media along the normal to the surface. In the range of small angles of beam incidence toward the boundary surface, the reflection coefficient remains constant [7], so the curvature of the lens does not affect the value of the reflection coefficient. The reflection coefficient ρ_k and the transmission coefficient $(1-\rho_k)$ in Eq. (13) through the interfaces k and $k+1$ of the media are determined by refractive indices of these media (n); under normal beam incidence, these dependences have the following form [7]:

$$\rho_{k,k+1} = \frac{(n_{k+1}-n_k)^2}{(n_{k+1}+n_k)^2}, \quad 1-\rho_{k,k+1} = \frac{4\cdot n_k \cdot n_{k+1}}{(n_{k+1}+n_k)^2}. \tag{14}$$

The Lms34LED-CG LED [10] and Lms36PD-CG PD [11] used in the sensor are made on the basis of semiconductor lattice heterostructure InAs with refractive coefficient of optical emission $n_1 = n_7 = n_{semicond} = n_{InAs} = 3.4$. The refraction coefficient of optical emission by air is $n_2 = n_4 = n_6 = n_{air} = 1$. As an optical material for the lenses (L_1 and L_2) of the sensor optical system (see Fig. 2), synthetic sapphire (Al_2O_3) is used; its refractive index ($n_3 = n_5 = n_{L_1} = n_{L_2}$) depends on the emission wavelength. In the working wavelength range of the sensor optoelectronic components (from 2.8 to 4.4 μm), the refractive index$n_{L_1} = n_{L_2}$ is in the range from 1.720 to 1.649 [7], which is no more than 5 %, therefore the change in this factor can be neglected, and value $n_{L_1} = n_{L_2}$=1.693 can be used in calculations. The transmission coefficient of the optical system, the structure of which is shown in Fig. 2, taking into account the optical emission losses calculated by Eq. (14), is equal to:

$$\begin{aligned}\tau_O &= (1-\rho_{1,2})\cdot(1-\rho_{2,3})\cdot(1-\rho_{3,4})\cdot \\ &\cdot(1-\rho_{4,5})\cdot(1-\rho_{5,6})\cdot(1-\rho_{6,7}) = \\ &= 0.702\cdot 0.934\cdot 0.934\cdot 0.934\cdot 0.934\cdot 0.702 = 0.375.\end{aligned} \tag{15}$$

Analysis of the obtained value τ_O led to the conclusion that emission flux losses when using materials with different optical properties in the sensor are no more than 37.5 %. The main optical power losses occur (see Fig. 2) at boundary surfaces 1 – 2 and 2 – 3 of the transmitting, as well as 5 – 6 and 6 – 7 of the receiving part of the sensor optical system.

Reduction in the value of these losses is possible due to the use of a volumetric coating of the corresponding shape of the LED and PD active elements. This coating should be an optically transparent material with refractive index (n_{glass}), whose value is close to the refractive index of the used semiconductor ($n_{semicond}$=n_{InAs}=3.4). This significantly increases the input and output ratio of optical emission. The advantage of this method lies in its simplicity and manufacturability, as well as in the capability to protect the LED and PD active elements from mechanical damage and environmental effects simultaneously. When covering the spaces between LED and L_1 (see 2 Fig. 2) and L_2 and PD (see 6 Fig. 2), the boundaries of sections 2 – 3 and 5 – 6 disappear. In this case, the coating of the optoelectronic sensor components serves as a lens (L_1 and L_2). The manufacturer of the LED and PD used in the sensor, based on the technology of their manufacture, proposed to use chalcogenide glass of As_2S_3 type with refractive index $n_2 = n_6 = n_{glass} = 2.42$ at a wavelength of 3.4 μm. Therefore, the transmission coefficient of the optical sensor circuit τ'_O (see Fig. 2), taking into account properties of the coatings used and the absence of the boundaries of sections 2 – 3 and 5 – 6, is calculated by the formula:

$$\tau'_O = (1-\rho_{1,2})\cdot(1-\rho_{2,4})\cdot(1-\rho_{4,6})\cdot(1-\rho_{6,7}) = 0.972\cdot 0.828\cdot 0.828\cdot 0.972 = 0.648, \quad (16)$$

which is 1.7 times more than in the optical system without coating of optoelectronic components of the sensor. Based on the theoretical studies and laboratory tests confirming them, we concluded that the use of LED of Lms34LED-CG type [10] and PD of Lms36PD-CG type [11] with chalcogenide glass covering of optoelectronic components, means at least 1.7 times less value of the basic error in methane concentration measurement.

3.2. Model of Spectral Adjustment of Optoelectronic Components

Efficiency of PD emission reception in the wavelength range of LED maximum intensity from λ_1 to λ_2 is estimated by the spectral matching coefficient (k_λ), determined by the following relation:

$$k_\lambda = \frac{\int_{\lambda_1}^{\lambda_2} S_{\mathrm{PD}}\cdot S_{\mathrm{LED}}\mathrm{d}\lambda}{\int_{\lambda_1}^{\lambda_2} S_{\mathrm{PD}}\mathrm{d}\lambda}, \quad (17)$$

where S_{PD} – normalized spectral response of the PD sensitivity; S_{LED} – normalized spectral density of the LED emission flux incident on the PD.

Figure 3 shows: 1– s_{PD} PD of Lms36PD-CG type, the values of which are established based on the results of experimental research of the manufacturer [11]; 2 – s_{PD} PD of Lms36PD-CG type, approximated by a polynomial with exponent 7, the relative mean square error of approximation does not exceed ±15 % in the wavelength range from 3.10 to 3.65 μm, which corresponds to the maximum emission intensity of the LED of Lms34LED-CG type; 6 – s_{PD} PD of Lms43PD-CG s_{PD} type, the values of which are established on the basis of the results of experimental research of the manufacturer [12]; 7 – s_{PD} PD of Lms43PD-CG type, approximated by a polynomial with exponent 7, the relative mean square error of approximation does not exceed ±8 % in the wavelength range from 3.10 to 3.65 μm, which corresponds to the maximum emission intensity of the LED of Lms34LED-CG type; 3 – transmission coefficient of the optical channel K_{OC} at $C_{\mathrm{CH_4}}$ =5 vol.%, T=298 K and P=101325 Pa; 4 – s_{LED} LED of Lms34LED-CG type, the values of which are established on the basis of the results of experimental research of the manufacturer [10]; 5 – s_{LED} LED of Lms34LED-CG type, approximated by the function:

$$S_{\mathrm{LED}} = e^{-r^2\cdot(\lambda-\lambda_0)^2}, \quad (18)$$

where λ_0, μm – central wavelength of the LED emission; r, μm^{-1} – half-width of the LED emission spectrum.

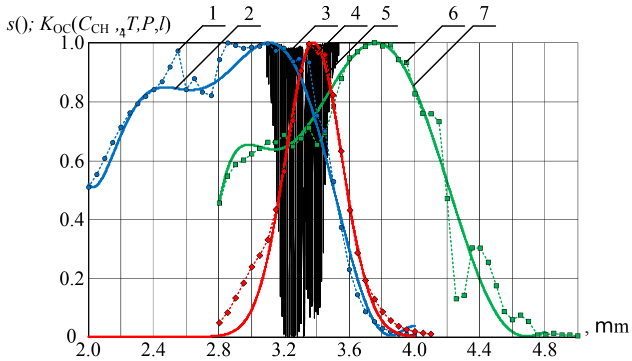

Fig. 3: K_{OC} where =5 vol.% (3) and normalized spectral characteristics of Lms34LED-CG LED (4 and 5), PD of Lms36PD-CG type (1 and 2) and PD of Lms43PD-CG type (6 and 7).

Values of the function parameters Eq. (18) λ_0=3.38 μm and r=4.05 μm^{-1} at the value of the relative standard uncertainty of approximating the results of experimental studies by s_{LED} function Eq. (18), whose value is no more than ±7 % in the range λ from 3.10 to 3.65 μm of LED maximum emission intensity.

The value of k_λ, according to the calculations performed by Eq. (17) and Eq. (18), in the wavelength range from 3.10 to 3.65 μm of the maximum emission intensity of Lms34LED-CG LED (see 5 Fig. 3) and Lms36PD-CG PD (see 2 Fig. 3) is 0.715, and Lms34LED-CG LED (see 5 Fig. 3) and Lms43PD-CG PD (see 7 Fig. 3) is 0.761. Based on the analysis of the conducted research, it has been established that the spectral adjustment coefficient of Lms34LED-CG LED with Lms43PD-CG PD is 6.5 % more compared to Lms34LED-CG LED and Lms36PD-CG PD, which, on the one hand, enables us to recommend the use of PD of Lms43PD-CG type in the sensor.

On the other hand, based on the results of additional theoretical and experimental studies, it was established that noise equivalent power of the output signal Lms43PD-CG ($4.8\cdot10^{-12}$ W·Hz$^{-0.5}$) [12] is 8 times higher than in Lms36PD-CG ($6.0\cdot10^{-13}$ W·Hz$^{-0.5}$) [11], and detection is respectively 5.1 times higher in Lms36PD-CG ($2.0\cdot10^{10}$ cm·Hz$^{0.5}$·W^{-1}), compared with Lms43PD-CG ($3.9\cdot10^{9}$ cm·Hz$^{0.5}$·W^{-1}). Therefore, the use of Lms43PD-CG PD in the optoelectronic sensor increases the value of the absolute error of methane concentration measurement by 8 times. Having performed simultaneous analysis of spectral adjusting of LED with PD, as well as noise properties of the PDs of Lms36PD-CG and Lms43PD-CG types, we recommend using the PD of Lms36PD-CG type in the optoelectronic sensor, has 6.5 % lower spectral compliance with the LED of Lms34LED-CG type, but 5.1 times higher detection than Lms43PD-CG.

3.3. Development of Spatial Adjustment Model

In real designs of optoelectronic sensors of concentration of gas components, it is difficult to reconcile geometric parameters of PDs and LEDs (see Fig. 4). Therefore, this factor is taken into account by the matching factor (k_{XY}), as a possible discrepancy between the area of the sensing element PD (S_{PD}) and the cross-sectional area of the optical emission flux (S_ϕ) at the PD installation place:

$$k_{XY=\frac{S_{PD}}{S_\phi}} = \frac{\phi_{\text{window PD}}}{\phi_{\text{plane PD}}} = \frac{\int_{a_1}^{a_2}\int_{b_1}^{b_2} Q\mathrm{d}y\mathrm{d}x}{\int\limits_{-\infty}^{\infty}\int\limits_{-\infty}^{\infty} Q\mathrm{d}y\mathrm{d}x}, \quad (19)$$

where Q – spatial density of the emission flux, which normally falls along the plane PD; a_1, a_2, b_1, b_2 –coordinates of the photodetector window in the XY coordinate system (the center of the coordinate system coincides with the intersection point of the ray axis and the PD plane); $\phi_{\text{plane PD}}$ – value of the optical emission flux, which falls on the plane PD; $\phi_{\text{window PD}}$ – part of the flow that enters the PD window.

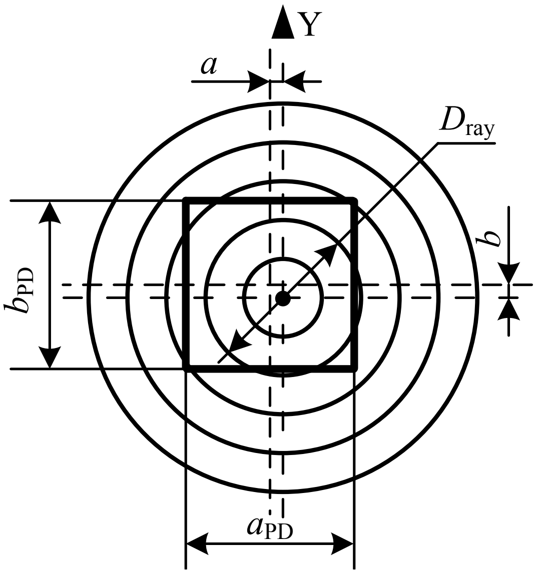

Fig. 4: Topographical plan for emission input into the PD window.

Spatial density of the emission flux incident on the normal to the PD plane is described by the function:

$$Q = Q_{\max}^2 \cdot q = Q_{\max}^2 \cdot \frac{r^2}{r^2 + (x^2 + y^2)}, \quad (20)$$

where $Q_{\max}$ - maximum value of the spatial emission flux density Q; q - normalized emission flux density; x and y - current coordinate values; r - half-width q, which is determined from the condition:

$$q\left(x = \frac{D_{ray}}{2}, y = 0\right) = \frac{r^2}{r^2 + \left(\frac{D_{ray}}{2}\right)} = 0.5, \quad (21)$$

where D_{ray}, mm – diameter of the LED beam.

As a result of solving Eq. (21), the value of the parameter $r = 0.5 \cdot D_{ray}$ is established. The largest value of $Q_{\max}$ in function Eq. (20) is determined from the condition:

$$\begin{aligned}\phi\left(C_{CH_4\ v} = 0\ ^{\text{vol.}\%}\right) &= \int\limits_{-\infty}^{\infty}\int\limits_{-\infty}^{\infty} Q_{\max}^2 \cdot q(x,y)\mathrm{d}y\mathrm{d}x \\ &= 4 \cdot Q_{\max}^2 \int\limits_{-\infty}^{\infty}\int\limits_{-\infty}^{\infty} q(x,y)\mathrm{d}y\mathrm{d}x.\end{aligned} \quad (22)$$

The value $\phi_{\text{plane PD}} = \phi\left(C_{CH_4\ v} = 0\ ^{\text{vol.}\%}\right)$ for functions Eq. (20) and Eq. (22) is determined at the maximum value of the emission flux. From Eq. (22) the value $Q_{\max}$ is set:

$$Q_{\max} = \sqrt{\frac{\phi\left(C_{CH_4} = 0\ ^{\text{vol.}\%}\right)}{4 \cdot \int\limits_0^{\infty}\int\limits_0^{\infty} q(x,y)\,\mathrm{d}y\mathrm{d}x}}. \quad (23)$$

The graph of efficiency changes of optical emission input into the PD window, which is estimated by k_{XY} according to Eq. (19), from the inconsistency of the X and Y coordinates of LED and PD optical axes (see Fig. 4) in the range of Δa and Δb changes from –10 mm to +10 mm is shown in Fig. 5. This range of changes Δa and Δb for Lms34LED-CG LED [10] and Lms36PD-CG PD [11] is twice the geometric dimension of the sensitive area $a_{PD} = b_{PD}$=5 mm with the beam diameter Lms34LED-CG D_{ray}=5 mm.

Having analysed the simulation results (see Fig. 5), we established that the maximum value of k_{XY} is 0.977 with inconsistency of the optical axes LED and PD by 0.5 mm in each of the coordinates. This error ratio is 10 % of the geometric dimensions of sensitive areas of the optoelectronic sensor component. If the inconsistency increases to 50 % of the geometric dimensions of the LED and PD areas, the value of k_{XY} reduces to 0.575, which is more than 42.5 % of the power losses and causes a practically proportional deterioration in the metrological characteristics of the sensor. The size of the error ratio between the optical axes LED and PD is recommended to provide no more than 20 % of the geometric dimensions of the sites of the optoelectronic components. At the same time, k_{XY}=0.912, which corresponds to no more than 8.8 % of the optical emission loss. This indicator depends on the quality of the alignment of the optical system, which should be carried out only in the industrial conditions of the LED and PD manufacturer. The sensor should be manufactured in

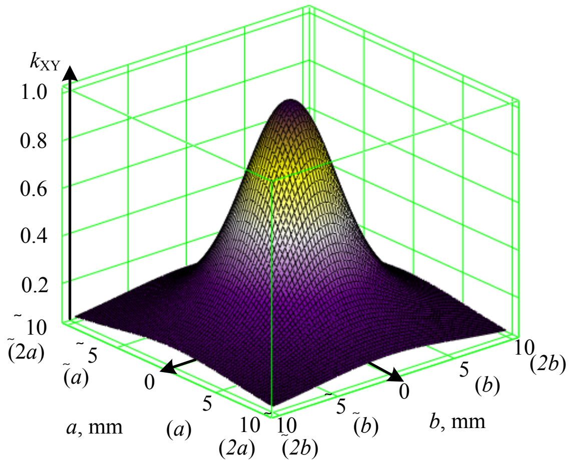

Fig. 5: Changes in the optical emission input coefficient to the PD window from the inconsistency of the LED and PD optical axes.

the form of a tube [13] with a regulated optical length and the necessary quality of alignment of its components.

3.4. Model of Losses at Modulation and Signal Processing

To improve metrological characteristics of the developed sensor, the authors [14] and [15] proposed to increase the LED output power by using electronic modulation of the supply current. For this purpose, we recommend increasing amplitude of current pulses to 1 A with a period of supply pulses T_{I}=2000 µsec with duration t_{i}=20 µsec, with on-line time ratio value q_{I}=100. When modulating with interruption of the optical flux ϕ_{LED}, which is proportional to the amplitude of the supply current (I_{LED}), signal power losses occur ($\phi_{0\mathrm{LED}}$), the value of which is taken into account with the coefficient:

$$k_{\mathrm{M1}} = \frac{\frac{1}{T_{\mathrm{I}_{\mathrm{LED}}}} \cdot \int\limits_{0}^{T_{\mathrm{I}}} \phi_{\mathrm{LED}} \mathrm{d}t}{\phi_{0\ \mathrm{LED}}} = \frac{t_{\mathrm{i}}}{T_{\mathrm{I}}} = \frac{1}{q_{\mathrm{I}}} = \frac{1}{100} = 0.01. \quad (24)$$

The numerator of Eq. (24) determines the average value of the optical emission flux. The value of this coefficient will decrease with increasing pulse sequence on-line time ratio of the LED supply current. Depending on the further processing of the sensor output signal, the value of which is proportional to $k_{\mathrm{M2}} \cdot \phi_{0\mathrm{LED}}$, only a part of the signal output power is used. Power losses due to limitation of the output signal spectrum of the sensor are taken into account by k_{M2}, and power losses during modulation can be taken into account by k_{M1}, hence:

$$k_{\mathrm{M}} = k_{\mathrm{M1}} \cdot k_{\mathrm{M2}}. \quad (25)$$

In Eq. (25), the coefficient k_{M1} determines the part of useful power used in the optoelectronic sensor relative to the power in the absence of modulation of the current supplying the LED.

The coefficient k_{M2} in Eq. (25) determines the way the modulated signal is processed. To increase the value of k_{M2}, we [14] and [15] proposed not to change the output signal spectrum of the sensor while it is being demodulated, but to measure its amplitude value using a Synchronous Detector (SD) [14] and [15]. For implementing this method, it is necessary to transmit a synchronization signal to the receiving part of the measuring system designed on the basis of the optoelectronic sensor, which contains information on the pulse sequence duration and its period. The use of SD makes it possible to maximize the value of k_{M2} to unity, and taking into account the relative error of the analog SD no more than ±5 %, the value of k_{M2} is 0.95. In this case, the value of the loss coefficient for modulation and processing of the sensor output signal is:

$$k_{\mathrm{M}} = k_{\mathrm{M1}} \cdot k_{\mathrm{M2}} = 1.00 \cdot 0.95 = 0.95. \quad (26)$$

The obtained value of k_{M} is the maximum with the chosen method of modulation and demodulation of the information measurement signal in the optoelectronic sensor of methane concentration.

3.5. Development of Emission Loss Model at its Input into the Photodetector Window

An important factor affecting the amount of optical power losses in the sensor is a diaphragming effect. It consists in forming a blind spot in the central part of the PD window (see Fig. 6), whereby only a part of the emission flux from the LED enters the PD window. The LED forms a spatial flow with circular symmetry in the perpendicular cross-section and maximum spatial density on its axis. This characteristic is the body of rotation and forms a directional pattern of the LED, which depends on the angle (φ) of deviation from its axis to the direction of emission propagation. In LED Lms34LED-CG the value of φ is no more than 8° [10].

Losses of optical emission from the LED at its input into the PD due to diaphragming is taken into account by k_{input}, which is equal to the ratio of the difference in the cross-sectional area of the PD (S_{PD}) and the created 'blind' spot ($S_{\mathrm{blind\ spot}}$) to the S_{PD}:

$$\begin{aligned} k_{\mathrm{input}} &= \frac{S_{\mathrm{PD}} - S_{\mathrm{blind\ spot}}}{S_{\mathrm{PD}}} = \\ &= \frac{D_{\mathrm{PD}}^2 - \left(2 \cdot l \cdot \tan\left(0.5 \cdot \varphi\right)\right)^2}{D_{\mathrm{PD}}^2}, \end{aligned} \quad (27)$$

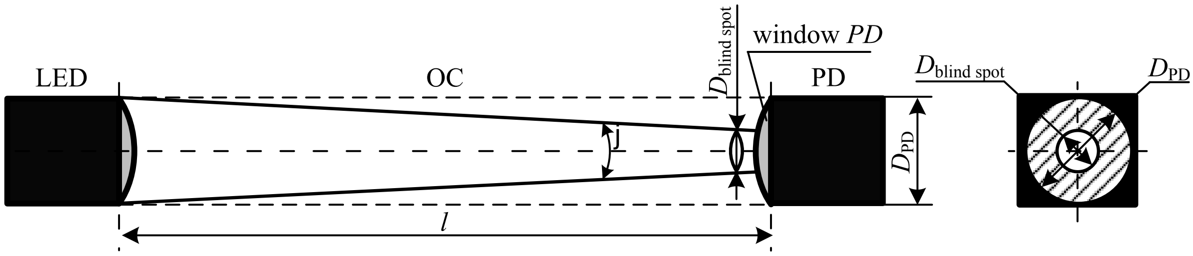

Fig. 6: Diagram of optical emission input from the LED to the PD window.

where D_{PD} – diameter of the input window of Lms36PD-CG PD equal 5 mm [11]; φ – angle of emission deviation from the axis of the LED in the direction of its propagation; $D_{\text{blind spot}}$ – diameter of the section of the 'blind' optical LED emission zone at the PD installation place (see Fig. 6), calculated by the formula: $D_{\text{blind spot}} = 2 \cdot l \cdot \tan(0.5 \cdot \varphi)$.

Having analysed the dependence Eq. (27), we concluded that as the length of the optical path (l) increases, the value of k_{input} decreases, while the power losses from the LED increase. When Lms34LED-CG LED is used with a value of $\varphi = 8°$ and the path length changes from 10 to 35 mm, kinput value decreases from 0.922 to 0.042, which corresponds to 7.8 to 95.8 % without taking into account the influence of changes in other destabilizing factors. On the one hand, the more l is, the greater the LED emission losses are. On the other hand, decrease in l leads to decrease in the informative value – the difference between K_{OC}, which is determined by Eq. (5), with the value of the measured concentration of $C_{CH_4\ v}$=0 $^{\text{vol.}}$% and K_{OC} at $C_{CH_4\ v}$=5 $^{\text{vol.}}$%:

$$\begin{aligned} \Delta K_{OC} = K_{OC}\left(C_{CH_4\ v} = 0\ ^{\text{vol.}}\%\right) \\ -K_{OC}\left(C_{CH_4\ v} = 5\ ^{\text{vol.}}\%\right). \end{aligned} \quad (28)$$

Reducing the OC path length from 35 mm to 10 mm reduces the value of ΔK_{OC} from 0.089 to 0.026, which leads to decrease in sensitivity and increase in the measurement error of the optoelectronic sensor of methane concentration. Therefore, taking into account the influence of the destabilizing factors under consideration, it is necessary to determine at what length of the OC path the maximum value of ΔK_{OC} calculated by Eq. (28) is ensured with minimum optical power losses or the maximum value of the optic-electronic efficiency of the methane concentration sensor, which is calculated by Eq. (8).

3.6. Recommendations for Improving the Sensor

Based on the results of mathematical modelling and experimental studies of the optoelectronic sensor of methane concentration, which confirm the adequacy of the developed prototypes, an estimate of its optoelectronic efficiency was performed. Without using the coatings of the optoelectronic components of the meter and without k_{input}, the value of η_{OE} is:

$$\tau_O \cdot k_\lambda \cdot k_{XY} \cdot k_M = 0.375 \cdot 0.715 \cdot 0.912 \cdot 0.95 = 0.232, \quad (29)$$

taking into account LED and PD covering with chalcogenide glass of As_2S_3 type is equal to:

$$\tau'_O \cdot k_\lambda \cdot k_{XY} \cdot k_M = 0.648 \cdot 0.715 \cdot 0.912 \cdot 0.95 = 0.401. \quad (30)$$

Based on the estimates of the optoelectronic efficiency without (τ_O) and with LED and PD covering (τ'_O) the following dependencies were established: ΔK_{OC} calculated according to Eq. (28) and η_{OE} according to Eq. (8) taking into account k_{input} according to Eq. (27) with the change of l in the range from 0 to 40 mm and the value of the LED emission pattern angle $\varphi = 8°$, which are shown in Fig. 7. The intersection points of the graphs τ_O (τ'_O) and ΔK_{OC} (see Fig. 7) determine the nominal lengths of the OC, at which the minimum losses of optical radiation and the maximum values of the informative parameter (ΔK_{OC}) are ensured.

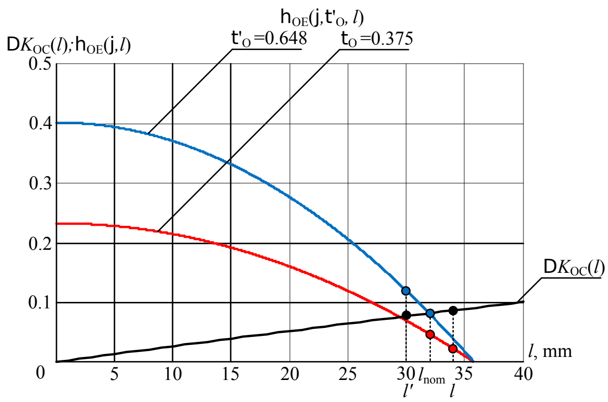

Fig. 7: Dependence of ΔK_{OC} and η_{OE} on changing the OC path length from 0 to 40 mm at $\varphi = 8°$.

Having analysed the obtained dependences (see Fig. 7), we established the nominal length of the optical channel (l_{nom}=32 mm) for ensuring minimum emission losses with the use of chalcogenide glass covering of the sensing elements of the optoelectronic sensor components:

$$\eta'_{\mathrm{OE}}\left(\varphi=8^\circ, l_{\mathrm{nom}}=32\ \mathrm{mm}\right)= \\ =\tau'_{\mathrm{O}} k_\lambda k_{\mathrm{XY}} k_{\mathrm{M}} k_{\mathrm{input}}\left(\varphi=8^\circ, l_{\mathrm{nom}}=32\ \mathrm{mm}\right)= \\ =0.080, \tag{31}$$

with maximum value of ΔK_{OC}=0.081. Without LED and PD covering, the value of optical-electronic efficiency is equal to:

$$\eta_{\mathrm{OE}}\left(\varphi=8^\circ, l_{\mathrm{nom}}=32\ \mathrm{mm}\right)= \\ =\tau_{\mathrm{O}} k_\lambda k_{\mathrm{XY}} k_{\mathrm{M}} k_{\mathrm{input}}\left(\varphi=8^\circ, l_{\mathrm{nom}}=32\ \mathrm{mm}\right)= \\ =0.046. \tag{32}$$

Based on these estimates, confirmed by results of our experimental studies of the developed optoelectronic sensor prototype for methane concentration measurement, we proved that the use of Lms34LED-CG LED [10] and Lms36PD-CG PD [11] with covering of sensitive elements with chalcogenide glass of As_2S_3 type allowed us to increase magnitude of optical-electronic efficiency 1.7 times compared with Lms34LED LED and Lms36PD PD previously used in the sensor without the appropriate covering.

The length of the optical path (l_{nom}=32 mm) was substantiated; the choice was made so that the value of optical emission losses in the channel would be minimum with the maximum value of the informative component. Based on the analysis of the research results, we recommend using the length of the OC path l'=30 mm (see Fig. 7), at which the value ΔK_{OC} decreases from 0.081 at l_{nom}=32 mm to 0.076 at l'=30 mm, which is 6.6 % of the information component signal losses, while the optical-electronic efficiency becomes 1.5 times higher – from 0.080 at l_{nom}=32 mm to 0.119 at l'=30 mm (see Fig. 7). The acceptable value of deviation of the OC length from l'=30 mm in the manufacture of the optoelectronic sensor is recommended to be chosen in the smaller direction, since the value of the information signal decreases up to 6.6 % with reduction of the base length by 2 mm, and the value η_{OE} increases by 1.5 times. The recommended deviation of the OC length from l'=30 mm should not be more than 1.0 mm.

To compare and analyse the results of mathematical modelling with experimental studies of the previously developed sensor prototypes [14] and [15], we propose to use a complex indicator (k'_{kompl}), which is equal to the product of optical-electronic sensor efficiency by the informative component of its output signal:

$$k'_{\mathrm{kompl}}= \\ =\eta'_{\mathrm{OE}}\left(\varphi=8^\circ, l'=30\ \mathrm{mm}\right)\cdot\Delta K_{\mathrm{OC}}\left(l'=30\ \mathrm{mm}\right)= \\ =0.119\cdot 0.076=9.04\cdot 10^{-3}. \tag{33}$$

In the previously developed prototypes of the optical-electronic sensor of methane concentration [14] and [15], the length of the optical path l=34 mm (see Fig. 7), as well as Lms34LED LED and Lms36PD PD without covering with chalcogenide glass, the value of the proposed indicator is:

$$k_{\mathrm{kompl}}= \\ =\eta_{\mathrm{OE}}\left(\varphi=8^\circ, l=34\ \mathrm{mm}\right)\cdot\Delta K_{\mathrm{OC}}\left(l=34\ \mathrm{mm}\right)= \\ =0.022\cdot 0.086=1.89\cdot 10^{-3}, \tag{34}$$

which is 4.8 times less than using the developed and proposed recommendations.

When studying the metrological characteristics of the previously developed prototype of the sensor, it was found that the value of the main absolute error in methane concentration measurement is not more than ±0.20 $^{\mathrm{vol.}}$%, which completely meets the regulated requirements for sensors [5], in the range from 0 to 5 $^{\mathrm{vol.}}$%. Analysis of the obtained results of mathematical modelling confirms a decrease in the magnitude of the measurement error of methane concentration by 4.8 times (±0.04 $^{\mathrm{vol.}}$% in the range from 0 to 5 $^{\mathrm{vol.}}$%) due to the use of the developed and sound recommendations. The obtained metrological characteristics of the improved optoelectronic sensor of methane concentration fully satisfy the requirements for mine conditions.

4. Conclusion

The mathematical model of the methane concentration sensor was developed and investigated; the model is based on optoelectronic efficiency, which takes into account such dominant destabilizing factors as the use of materials with different optical properties, spectral and spatial adjustment of the optoelectronic sensor components, losses at modulation and signal processing, as well as dispersion of the optical emission flux with increasing path length.

Analysis of simulation results confirmed by experimental studies of the optoelectronic sensor of methane concentration, recommendations for improving its design parameters were substantiated and developed. The use of a light-emitting diode of Lms34LED-CG type and a photodiode of the Lms36PD-CG type with spectral and spatial adjustment of characteristics, as well as their covering with chalcogenide glass of

As_2S_3 type, increases the optoelectronic efficiency by 1.7 times. When choosing one of the main design parameters of the optoelectronic sensor, namely the length of the optical path, which is less than 30 mm, the values of the minimum emission losses in the optical channel were justified and established at the maximum value of the informative parameter, which is the value of optical emission absorption by the measured methane concentration.

Implementation of the proposed recommendations while designing the optoelectronic sensor allowed us to provide the value of the main absolute error of methane concentration measurement no more than ± 0.04 $^{\mathrm{vol.}}$% with the regulated value of no more than ± 0.20 $^{\mathrm{vol.}}$% in the range from 0 to ± 5 $^{\mathrm{vol.}}$%. The obtained result significantly exceeds the accuracy of existing prototypes of the methane concentration sensor for the conditions of mine atmosphere.

References

[1] KVENVOLDEN, K. A. and B. W. ROGERS. Gaia's breath—global methane exhalations. *Marine and Petroleum Geology*. 2005, vol. 22, iss. 4, pp. 579–590. ISSN 0264-8172. DOI: 10.1016/j.marpetgeo.2004.08.004.

[2] MASSIE, C., G. STEWART, G. MCGREGOR and J. R. GILCHRIST. Design of a portable optical sensor for methane gas detection. *Sensors and Actuators B: Chemical*. 2006, vol. 113, iss. 2, pp. 830–836. ISSN 0925-4005. DOI: 10.1016/j.snb.2005.03.105.

[3] YU, K., C. WU and Z. WANG. Optical Methane Sensor Based on a Fiber Loop at 1665 nm. *IEEE Sensors Journal*. 2010, vol. 10, iss. 3, pp. 728–731. ISSN 1530-437X. DOI: 10.1109/jsen.2009.2033261.

[4] VOVNA, O., A. ZORI and I. LAKTIONOV. Improving efficiency of information measurement system of coal mine air gas protection. *Mining of Mineral Deposits*. 2017, vol. 11, iss. 1, pp. 23–30. ISSN 2415-3435. DOI: 10.15407/mining11.01.023.

[5] DSTU GOST. *The mine's gas-analytical instruments. General requirements, test methods*. Kiev: Derzhspozhivstandart, 2009.

[6] WARDLE, B. *Principles and Applications of Photochemistry*. Hoboken: John Wiley and Sons Ltd, 2010. ISBN 04-700-1494-6.

[7] ZUEV, V. E. *Laser beam in the atmosphere*. New York: Plenum Publishing Corporation, 1982. ISBN 03-061-0967-0.

[8] BROWN, L. R., D. C. BENNER and J. P. CHAMPION. Methane line parameters in HITRAN. *Journal of Quantitative Spectroscopy and Radiative Transfer*. 2003, vol. 82, iss. 1, pp. 219–238. ISSN 0022-4073. DOI: 10.1016/S0022-4073(03)00155-9.

[9] SCHUBERT, E. F. *Light-Emitting Diodes*. 2nd ed. New York: Cambridge University Press, 2006. ISBN 05-218-6538-7.

[10] LED MICROSENSOR. LEDs with a glass covering: Lms34LED-CG. *LED Microsensor NT LLC* [online]. 2018. Available at: `http://lmsnt.com/datasheets/Standard%20chip/Lms34LED-CG/Lms34LED-CG_TO18_rev240317.pdf`.

[11] LED MICROSENSOR. PDs with a glass covering: Lms36PD-CG. *LED Microsensor NT LLC* [online]. 2018. Available at: `http://lmsnt.com/datasheets/PD/Lms36PD-CG/Lms36PD-05-CG_Series_rev240317.pdf`.

[12] LED MICROSENSOR. PDs with a glass covering: Lms43PD-CG. *LED Microsensor NT LLC* [online]. 2018. Available at: `http://lmsnt.com/datasheets/PD/Lms43PD-CG/Lms43PD-05-CG_Series_rev240317.pdf`.

[13] LED MICROSENSOR. Evaluation Kits: MDS-5 CH4 Detection System. *LED Microsensor NT LLC* [online]. 2018. Available at: `http://lmsnt.com/datasheets/Electronics/MDS-5_en-250516.pdf`.

[14] VOVNA, O. V., A. A. ZORI and S. S. LAKTIONOV. Hardware and software method of the output signal temperature drift compensating of the methane concentration optical meter. *Technical Electrodynamics*. 2017, vol. 4, iss. 1, pp. 86–92. ISSN 2218-1903.

[15] VOVNA, O., S. ZORI and I. LAKTIONOV. Design of an optical methane concentration meter, invariant to temperature changes of mine atmosphere. In: *International Conference on Modern Electrical and Energy Systems (MEES)*. Kremenchuk: IEEE, 2017, pp. 408–411. ISBN 978-1-5386-1750-2. DOI: 10.1109/MEES.2017.8248946.

About Authors

Oleksandr Volodymyrovych VOVNA was born in Pavlivka, Donetsk region, Ukraine, in 1979. He received his master's degree in electronic systems from Donetsk National Technical University in 2004, a Ph.D. in engineering (2009) and a doctorate in engineering (2015), majoring in computer systems and components from the State Higher Education Institution Donetsk National Technical University (SHEI DonNTU). Since 2017 he has been working as Head of the Department of Electronic Engineering of the SHEI DonNTU. His research interests include development of methods and tools to improve the accuracy and speed of information and measurement systems for concentration of gas components for high explosive conditions of industrial enterprises. He is the author of 4 monographs, 9 textbooks and teaching aids, 120 scientific articles, 27 patents of Ukraine for inventions and utility models.

Ivan Serhiiovych LAKTIONOV was born in Snizhne, Donetsk region, Ukraine, in 1988. He received a master's degree in electronic systems from Donetsk National Technical University in 2012, a Ph.D. in engineering (2015), majoring in computer systems and components from the State Higher Education Institution Donetsk National Technical University (SHEI DonNTU). Since 2016 he has been working as an associate professor of the Department of Electronic Engineering of the State Higher Education Institution DonNTU. His research interests include development of advanced technologies for improving efficiency and informativeness of computerized monitoring and control of microclimate parameters of industrial greenhouses. He is the author of 1 monograph, 2 manuals, 50 scientific articles.

Anatolii Anatoliiovych ZORI was born in Donetsk, Ukraine, in 1941. He received the qualification of an electrical engineer in automatics and telemechanics from Donetsk Polytechnic Institute in 1964, the scientific degree of candidate of technica l sciences (1972) from All-Union Scientific Research Institute of Metrology named after Mendeleyev and a doctorate in information and measurement systems (1992) from St. Petersburg Electrotechnical Institute named after Ulyanov (Lenin). From 1993 to 2017 he worked as the Head of the Department of Electronic Engineering, and since 2017 he has been a professor of the Department of Electronic Engineering the State Higher Education Institution Donetsk National Technical University. His research interests include improving accuracy, speed and reliability of information and measurement systems for concentration of gas components in high explosive atmosphere. He is the author of 12 monographs, 37 textbooks and teaching aids, 260 scientific articles, 70 copyright certificates and patents for inventions.

Ramin Nizamiiovych AKHMEDOV was born in Donetsk, Ukraine, in 1992. He received his master's degree in electronic systems from Donetsk National Technical University in 2015. Since 2015 he has worked as a teaching assistant of the Department of Electronic Engineering of the State Higher Education Institution Donetsk National Technical University (Pokrovsk, Ukraine). In 2015 he became a postgraduate student at the Department of Electronic Engineering of the State Higher Educational Institution Donetsk National Technical University (Pokrovsk, Ukraine), specializing in computer systems and components. His research interests include development of methods and tools of improving accuracy and speed of information measurement systems of concentration of gas components for high explosive conditions of industrial enterprises, development of automation systems in accordance with industry 4.0 standard.